Solar Energy Materials & Solar Cells 144 (2016) 445–450

Contents lists available at ScienceDirect

Solar Energy Materials & Solar Cells

journal homepage: www.elsevier.com/locate/solmat

The oxidation effect of a Mo back contact on Cu(In,Ga)(Se,S)$_2$ thin-film solar modules

Junggyu Nam [a], Yoonmook Kang [b], Dongseop Kim [a], Dohyun Baek [a], Dongho Lee [a,*], JungYup Yang [a,*]

[a] PV Development Team, Energy Solution Business Division, Samsung SDI, 467, Beonyeong-ro, Seobuk-gu, Cheonan-si, Chungcheongnam-do 331-330, Republic of Korea

[b] Green School, Graduate school of Energy and Environment, 145 Anam-ro, Seongbuk-gu, Seoul 136-713, Republic of Korea

ARTICLE INFO

Article history:
Received 5 April 2015
Received in revised form
1 July 2015
Accepted 24 September 2015

Keywords:
Mo back contact
Mo oxidation
CIGSS module
Pattern
Na effect

ABSTRACT

We investigated the surface properties of a Mo back contact for large-area thin-film solar modules with high efficiency and good adhesion between Mo and the absorber layer. It was determined that the appropriate surface properties of Mo would improve the efficiency from 10% to above 15.0 ± 0.21% and narrow the efficiency distribution in large-area modules. The Mo back contact was annealed at various temperatures between room temperature and 230 °C in air to control the amount of sodium diffusing from the soda-lime glass substrate during selenization and sulfurization, and to improve the uniformity of the unit cell. Before the heat treatment, the amount of sodium in the patterned area of the unit cell was more than 10 times of that in the central area of the cell. The patterned region with higher Na content had smaller grains than those in the central area with less Na, resulting in many peel-offs and shunting paths. The difference in sodium content was reduced after heat treatment. The optimized surface oxide of the Mo back contact had a thickness of around 3–5 nm and consisted of the MoO_3 phase. The grain boundary of Mo columnar structure near the surface consisted of the oxide layer.

1. Introduction

The Mo back contact plays important roles in a solar cell, such as the collector of generated carriers and controller of the path of Na diffusion from a soda-lime glass substrate [1–4]. In a Cu(In,Ga)(Se,S)$_2$ (CIGSS) thin-film solar cell prepared by the H_2Se–H_2S reacting gas, the metal back contact should be resistant against the Se reaction in a hydrogen atmosphere during high-temperature selenization. A Mo back contact is commonly used because Mo has an appropriately high work function for an ohmic contact and can resist etching in a high-temperature process sequence. The Mo compounds produced in the process, such as $MoSe_2$, MoS_2, or Mo(Se,S)$_2$, have the appropriate lubricating property to assist sliding of the scribe needle [4–7]. $MoSe_2$ offers the advantage of being able to reduce the resistance between the CIGSS layer and Mo back contact with an ohmic contact [8–10]. However, $MoSe_2$ and MoS_2 are semiconductors with direct bandgaps, and if values of their layer thickness increase beyond hundreds of nanometers, the series resistance will be increased, especially for MoS_2 [11]. It has been reported that the properties and qualities of the back contact may depend on the surface conditions of the Mo layer, such as the oxidation state of the surface [11,12].

In this report, we focus on the advantages of the thin Mo oxide layer on the surface of the Mo contact for fabricating monolithic thin-film CIGSS solar modules. It is well known that many peel-offs can be found at the CIGSS–Mo interface near P1 patterns and in the middle of the cell if there is an oversupply of Na to the CIGSS absorber thin film. We will show the peel-offs have several origins in a large-area module, and we will discuss the process used to reduce such peel-offs. We will also present an analysis of thin-film properties obtained by secondary ion mass spectroscopy (SIMS), X-ray photoelectron spectroscopy (XPS), transmission electron microscopy (TEM), scanning electron microscopy (SEM), and shunt infrared (IR) imaging.

2. Experimental details

Thin films of CIGSS were prepared by sputtering and sequential selenization in a H_2Se (99.99%, 4N) atmosphere and sulfurization

Abbreviations: BZO, boron-doped zinc oxide; CBD, chemical bath deposition; CIGSS, copper–indium–gallium–sulfur selenide, Cu(In,Ga)(Se,S)$_2$; FF, fill factor; IR imaging, infrared imaging; LPCVD, low-pressure chemical vapor deposition; SEM, scanning electron microscopy; SIMS, secondary ion mass spectroscopy; TCO, transparent conductive oxide; TEM, transmission electron microscopy; XPS, X-ray photoelectron spectroscopy

* Corresponding authors.
E-mail addresses: dhlee0333@gmail.com (D. Lee), jungyupyang@gmail.com (J. Yang).

http://dx.doi.org/10.1016/j.solmat.2015.09.035
0927-0248/

in a H_2S (99.99%, 4N) atmosphere with N_2 in the furnace. A Cu–Ga–In metal alloy thin film was first deposited by DC magnetron sputtering with a rotary target before it was placed in a reaction furnace for sequential processing. The thickness of the thin film was controlled to adjust for the final CIGSS layer thickness after the processes. The back contact Mo layer was deposited by DC magnetron sputtering before the precursor thin film was deposited on the soda-lime glass substrate, which had a high strain point at temperatures above 600 °C when compared with normal soda-lime glass. For a monolithically integrated solar module, we scribed the Mo layer with a high-power laser for the first pattern (P1). The P1 width and adjacent P1 scribing were optimized based on the desired current density and transparent conductive oxide (TCO) thickness and quality. The oxidation of the Mo back contact was performed in air in a convection oven at several temperatures between room temperature and 230 °C for 20 min after P1 laser patterning. For the analysis of properties of the oxidized surface film, we deposited a capping layer on the Mo thin film to exclude the effect of the atmosphere before and after oxidation in the furnace. The buffer layer for reducing the number of shunting paths and increasing the interface quality was grown on the absorber layer via chemical bath deposition (CBD). The ZnS(O,OH)-based buffer layer was deposited using chemical sources such as $ZnSO_4$, NH_4OH, and thiourea dissolved in deionized (DI) water for 15 min. After the CBD process, mechanical scribing for the second pattern (P2) was performed to establish series connection between the unit cells isolated by P1. The gap between P1 and P2 was minimized to reduce the dead area in the total module area. Boron-doped ZnO (BZO) was deposited on the CBD buffer layer as a TCO window layer via low-pressure chemical vapor deposition (LPCVD). The final step of cutting the TCO layer to isolate the unit cell for modularization was carried out by mechanical scribing of the third pattern (P3).

The morphology of the thin film near the patterns was analyzed by SEM, and the electric properties were examined by reverse-biased shunt IR imaging. The depth profile of the thin film before and after oxidation was compared by SIMS. The morphologies of non-oxidized and oxidized Mo layers were also analyzed by XPS and TEM by measuring the layer thickness and characterizing the phase of the thin oxide layer. The efficiency of the prepared large-area modules was checked under calibrated AM 1.5G illumination in our pilot line.

3. Results and discussion

We performed precise electrical and physical analyses to investigate the direct contacts within this solar device. A shunt IR image of the module and the optical and shunt IR images of a cell in the CIGSS module are shown in Fig. 1(a)–(c), respectively. Many red spots are visible in Fig. 1(a), which depend on the direct contact between the Mo back contact and TCO layer when the CIGSS layer peeled off from the Mo back contact during processing. The shunt IR image shows that the heat originated from the ohmic contact in reverse biasing on the p–n junction of the solar device. This kind of ohmic contact creates shunting paths in real-life application and should be removed. The points P, C, and E in Fig. 1(b) and (c) indicate the range of patterns, the center of a cell, and the intermediate range between P and C, respectively. The optical image in Fig. 1(b) shows a different color at each site, while the electron microscope reverse-biased shunt IR image in Fig. 1(c) shows red spots at the center of each cell when measured at high resolution. During the preparation of the monolithic thin-film CIGSS solar module, when the heat treatment was performed to synthesize the absorber ($CIGSe_2$ or CIGSS) layer at high temperature, alkali elements such as Na and K were transported from the glass substrate into the CIGSS absorber layer through the Mo back contact [14–16]. In general, a larger quantity of the elements should be detected near the patterns because they were removed by the laser source for isolation from the Mo back contact. Other researchers have reported the effect of sodium from the point of view of grain growth and the crystallization [17–20], as well as the stability and passivation of the absorber layer [21–25]. We, on the other hand, focus on harmful effects in this report, such as the presence of excess Na as the cause of the peel-offs between the Mo back contact and absorber.

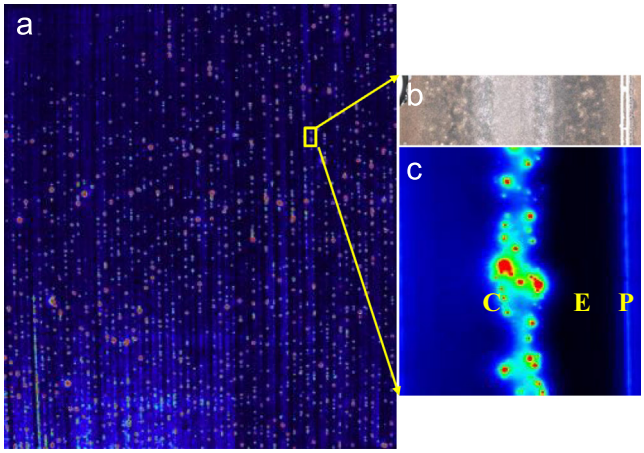

Fig. 1. Images of shunt IR (a) in CIGS module at low resolution and (b) in a unit cell of CIGS module at high resolution. (b) Optical image at the same position where (c) was obtained. The red spots show the ohmic contact at the unit cell. (For interpretation of the references to color in this figure legend, the reader is referred to the web version of this article.)

As mentioned earlier, to elucidate the basic reason for the difference in morphology of the three regions, we performed SEM analysis at points, C, E, and P. Fig. 2 describes cross-sectional SEM images of the film at these points. The grain size at point C was larger than those at points E and P, which were similar to each other. While points E and P had many voids between Mo and the CIGSS layer, none of them were observed at point C. Fig. 2(c) shows the regular voids generated by sputtering and sequential processing due to the expansion of the metal precursor and the reaction rate. The image of E in Fig. 2(b) depicts the larger voids with an irregular size. Fig. 3 shows the top-view of the same area measured by SEM at high resolution. In Fig. 3(a), the P region had a flat and smooth surface and the E region had irregularities on the surface. Many cavities were created by the CIGSS layer peeling off from the Mo back contact in the C region, as shown Fig. 3(b). It could be assumed that the difference in brightness in the three regions in Fig. 1(b) stemmed from the difference in reflection at the CIGSS surface as a result of the surface roughness. Based on these results, it appears that the ohmic contacts were created when the CIGSS layer peeled off from the Mo back contact at many points during selenization and sulfurization, and then TCO was deposited on the resulting cavities. To determine the reason for the peel-offs from the Mo back contact, we made the following assumptions: the difference in morphology was caused by the amount of transferred materials from the glass substrate; the peel-off at point C and the shape of embossing at point E originated from the difference in stress in different regions of the thin film owing to the different morphologies, such as grain size and void shape, in the regions. We first analyzed the Mo thin film to evaluate the validity of our assumptions at each point. Fig. 4 shows that a larger amount of surface oxygen resided at point P than point C. Since oxygen can assist the diffusion of alkali metals [1,26–29], the constituent elements of the absorber could have been changed after selenization. Although the above assumption has not been confirmed and more investigation is needed, we can make the following deductions: (1) The laser source for P1